

Seeing and Knowing in the Wild: Open-domain Visual Entity Recognition with Large-scale Knowledge Graphs via Contrastive Learning

Hongkuan Zhou^{1,2}, Lavdim Halilaj¹, Sebastian Monka¹, Stefan Schmid¹,
Yuqicheng Zhu^{1,2}, Jingcheng Wu², Nadeem Nazer^{1,4}, Steffen Staab^{2,3}

¹Corporate Research, Robert Bosch GmbH, Renningen, Germany

²University of Stuttgart, Stuttgart, Germany

³University of Southampton, Southampton, UK

⁴Otto-von-Guericke-University Magdeburg, Magdeburg, Germany

hongkuan.zhou@de.bosch.com

Abstract

Open-domain visual entity recognition aims to identify and link entities depicted in images to a vast and evolving set of real-world concepts, such as those found in Wikidata. Unlike conventional classification tasks with fixed label sets, it operates under open-set conditions, where most target entities are unseen during training and exhibit long-tail distributions. This makes the task inherently challenging due to limited supervision, high visual ambiguity, and the need for semantic disambiguation. We propose a **Knowledge-guided Contrastive Learning** (KnowCoL) framework that combines both images and text descriptions into a shared semantic space grounded by structured information from Wikidata. By abstracting visual and textual inputs to a conceptual level, the model leverages entity descriptions, type hierarchies, and relational context to support zero-shot entity recognition. We evaluate our approach on the OVEN benchmark, a large-scale open-domain visual recognition dataset with Wikidata IDs as the label space. Our experiments show that using visual, textual, and structured knowledge greatly improves accuracy, especially for rare and unseen entities. Our smallest model improves the accuracy on unseen entities by 10.5% compared to the state-of-the-art, despite being $35\times$ smaller.

Code — <https://github.com/hk-zh/KnowCoL>

Introduction

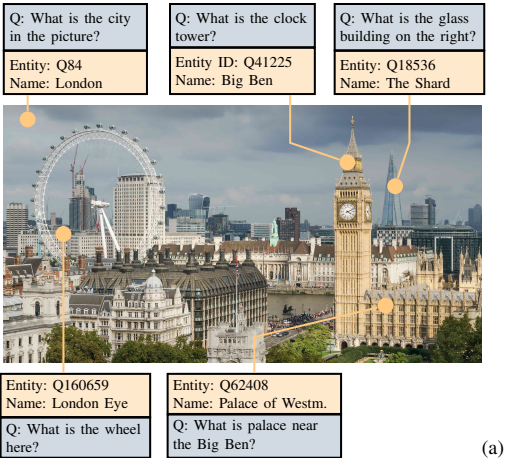
The ability to recognize and identify visual entities in the open world is a critical milestone for scalable computer vision systems. In contrast to traditional classification tasks that depend on a fixed set of categories, open-world visual entity recognition seeks to recognize and link images to a vast and evolving universe of real-world entities, such as specific landmarks, artworks, biological species, or public figures. The recently introduced Open-domain Visual Entity recognitioN (OVEN) benchmark (Hu et al. 2023) challenges models to link images and accompanying text query (specifying the intent of the image) to the correct Wikidata entities,¹ identified by its unique QID. A few examples of the OVEN-based tasks are shown in Figure 1a.

¹We consistently use the term **entity** to refer to uniquely identifiable real-world concepts in Wikidata (e.g. Albert Einstein (Q937) and Golden Retriever (Q38686)), which differs from the typical usage of **class**, denoting categories within a predefined set.

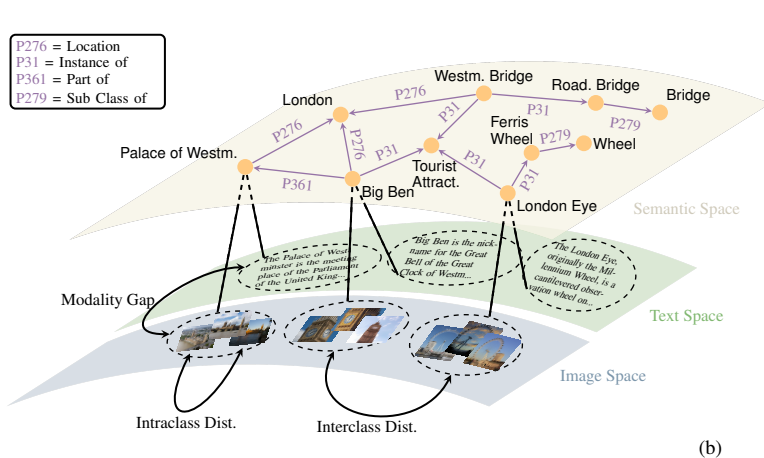
Previous approaches addressing open-world visual entity recognition typically adopt a dual-encoder paradigm, which aligns visual representations with textual descriptions of corresponding entities. CLIP2CLIP and CLIPFusion (Hu et al. 2023) include the information of the lead image(s) of the entities into the training pipeline for a better alignment of different modalities. Recently, researchers (Hu et al. 2023; Caron et al. 2024; Xiao et al. 2024) have developed *two-step* approaches which leverage generative language models, such as PaLI (Chen et al. 2023), GIT (Wang et al. 2022), and Vicuna (Zheng et al. 2023), to generate textual labels of images and then utilize search algorithms (e.g. BM25 (Robertson, Walker, and Hancock-Beaulieu 1995)) to identify entities whose names closely match these predicted labels.

Despite the progress, this task remains fundamentally challenging. First, the label space is extremely large and long-tailed, encompassing millions of entities, many of which are rare or entirely unseen during training. Second, existing visual classifiers treat entities as isolated labels, ignoring the wealth of semantic relationships and factual knowledge that exist between entities. These limitations hinder generalization, especially in zero-shot settings, where the model must recognize entities it has never encountered during training. Third, a key drawback of the two-step generative approaches is the *information loss* incurred when converting rich visual content into simplified textual labels, leading to semantic ambiguity (Sevgili et al. 2022; Bouarroudj, Boufaïda, and Bellatreche 2022) when conducting BM25 search algorithms based on the predicted textual labels to find the final entity. Entities with similar or identical textual labels may represent fundamentally different concepts. For instance, “Mercury” can denote either the innermost planet of our Solar System or the liquid metal with chemical symbol Hg (atomic number 80), showing how simple text matching cannot distinguish these distinct meanings.

We propose that open-domain visual entity recognition should move beyond superficial recognition toward semantic-level understanding. This involves abstracting both images and textual description into a shared conceptual space with rich structural knowledge among entities (cf. Figure 1b). In this view, recognition is not simply matching visual features to entity names, but of aligning image content with structured, contextualized knowledge about the en-



(a)



(b)

Figure 1: (a) The open-domain visual entity recognition task aims to link an image and a text query to a corresponding Wikidata entity. The text query expresses the intent to the image. (b) Both visual and textual inputs can be mapped to a shared semantic space enriched with structured knowledge, such as entity relations (e.g., instance-of, part-of, subclass-of) from Wikidata. Leveraging this additional knowledge source enables contextual reasoning and effective disambiguation of entities.

ties depicted. Available knowledge graphs (KGs), such as Wikidata, which offers a rich and structured representation of hierarchical and association relations for millions of real-world entities, can be leveraged to achieve this.

We present **Knowledge-Guided Contrastive Learning** (KnowCoL), an approach for open-domain visual entity recognition. Input images and candidate entities' descriptions and/or lead images are projected into a shared semantic embedding space, structured with the prior knowledge from the KG. This enables zero-shot recognition by allowing the model to generalize from seen to unseen entities based on semantic similarity, while also supporting entity disambiguation via knowledge-informed representations. KnowCoL is based on a dual-encoder paradigm, eliminating the information loss in the process of conversion in the two-step approaches. We evaluate our approach on the OVEN benchmark. Our contributions are as follows:

1. We present a dual-encoder approach for the open-domain visual entity recognition task that leverages external knowledge from both Wikidata and Wikipedia to enable a better representation of images and text descriptions.
2. We investigate the impact of different forms of external knowledge (including lead images) and different relations between entities on the recognition performance.
3. Our approach demonstrates strong zero-shot generalization on the OVEN benchmark, showing that incorporating external knowledge significantly improves entity recognition performance of unseen entities by 10.5%, even with models that are $35\times$ smaller.

Preliminary

Contrastive Loss

Contrastive loss is a widely used objective in representation learning, particularly in contexts such as metric learning, image-text alignment, and self-supervised learning. Given

two sets of embeddings $A = \{a_i\}_{i=1}^N$ and $B = \{b_i\}_{i=1}^N$, where (a_i, b_i) is a positive (matching) pair and $\forall (a_i, b_j), j \neq i$, is a negative pair, we define the contrastive loss as:

$$\ell(A, B) = -\frac{1}{N} \sum_{i=1}^N \log \frac{\exp(\text{sim}(a_i, b_i)/\tau)}{\sum_{j=1}^N \exp(\text{sim}(a_i, b_j)/\tau)}, \quad (1)$$

where $\text{sim}(\cdot, \cdot)$ denotes the similarity function, τ is a temperature parameter controlling the softness of the similarity distribution, and N is the set size. Common similarity functions include cosine similarity and Euclidean distance-based similarity. Specifically, the symmetric contrastive loss can be defined as,

$$\ell_{\text{sym}}(A, B) = \frac{1}{2} (\ell(A, B) + \ell(B, A)), \quad (2)$$

which encourages mutual alignment, and it is widely used in various models like CLIP.

Wikidata Knowledge Graph

Wikidata is a collaboratively-maintained, multilingual knowledge graph that can be formalised as the directed graph $\mathcal{G} = (\mathcal{E}, \mathcal{R}, \mathcal{T})$, where \mathcal{E} is the set of entities (called items and uniquely referenced by "Q-identifiers" (QIDs), e.g., Q42 for Douglas Adams), \mathcal{R} is the set of relation types (called properties and referenced by "P-identifiers" (PIDs), e.g., P31 for instance of), and $\mathcal{T} \subseteq \mathcal{E} \times \mathcal{R} \times \mathcal{E}$ is the set of knowledge triples (e_1, r, e_2) stating that subject entity e_1 is linked to object entity e_2 via property r . As of 2025, Wikidata KG contains more than 100 million entities, 12,000 properties, and 10 billion triples and is growing daily through human and bot contributions.

Wikipedia Knowledge Base

Wikipedia is a collaboratively edited, multilingual encyclopedia whose every article is linked to a unique Wikidata

QID. This tight coupling lets each page serve as a multi-modal hub: rich encyclopedic text is paired with lead images that provide both descriptive and visual context for the corresponding entity in the Wikidata KG.

Related Work

Zero-Shot Classification

Open-world recognition is closely related to zero-shot learning (ZSL), where models must recognize classes with no training images by relying on auxiliary information.

Early approaches (Farhadi et al. 2009; Lampert, Nickisch, and Harmeling 2009) introduced human-defined attributes as intermediate semantic representations for recognition of unseen classes. Later methods moved toward unsupervised semantic embeddings derived from text corpora (Socher et al. 2013; Frome et al. 2013; Norouzi et al. 2014). These dual-encoder or projection-based approaches have proven that aligning images with distributed text representations enables zero-shot recognition at scale. Vision-language pre-training has greatly advanced this paradigm. A well-known example is CLIP (Radford et al. 2021), which is trained on 400 million image-text pairs to learn a joint embedding space for images and natural language. By encoding an image and a candidate label (or description) into the same space, CLIP can directly measure their compatibility, essentially performing zero-shot classification by ranking labels. CLIP has wide applications in visual inspection (Jeong et al. 2023; Sadikaj et al. 2025) and robotics (Zhou et al. 2023, 2024a; Yao et al. 2025).

Another line of zero-shot research uses large-scale generative models to bridge the gap to unseen classes. Instead of directly mapping images to text semantics, these generative approaches output the entity names based on given images and then link the entity names to the categories (two-step approach). For instance, Hu et al. (2023) use PaLI and BLIP-v2 (Li et al. 2023a) on the OVEN benchmark to make the model predict the entity name and then uses the BM25 search algorithm to find the closest label in the label space of Wikidata ids. Instead of generating entity names, GERALD (Caron et al. 2024) generates the semantic and discriminative “code” to identify entities. Auto-VER (Xiao et al. 2024) combines contrastive learning with generative models to enhance the ability to distinguish similar entities within a vast label space. Unlike dual-encoder approaches, two-step generative methods output text conditioned on images and then match them to labels in the label space. This introduces semantic ambiguity, as generated outputs may be correct lexically but vague or incomplete semantically.

Knowledge Graphs for Visual Entity Recognition

Many studies have explored incorporating knowledge into vision-and-language tasks (Monka, Halilaj, and Rettinger 2022), including visual question answering (Chang et al. 2022; Chen et al. 2021) and entity-aware image captioning (Biten et al. 2019). For visual entity recognition task, Wang, Ye, and Gupta (2018) and Kampffmeyer et al. (2019) use semantic embeddings and categorical relationships from

KGs through graph convolution networks for zero-shot prediction. Li et al. (2023b) augments few-shot image recognition by introducing auxiliary semantic prior knowledge and propagating knowledge among categories via a semantic-visual mapping. KG-NN (Monka et al. 2021) combines prior knowledge encoded in KGs with visual representations to enhance generalization under distribution shifts, and KGV (Zhou et al. 2024b) demonstrates that the integration of richer multi-modal priors can further improve performance. Instead of relying on small domain-specific knowledge graphs, our approach is the first to leverage a large-scale knowledge graph for open-domain visual entity recognition, demonstrating strong scalability potential.

Methodology

Our goal is to integrate the rich, structured knowledge from Wikidata into the training pipeline. To achieve this, we align knowledge graph embeddings (KGEs), image embeddings, and text embeddings within a shared latent space, enabling the structured knowledge captured by the KGEs to be effectively injected into the latent space’s representation. A framework overview can be seen in Figure 2.

Problem Definition

Let \mathcal{E} be the set of Wikidata entities identified by QIDs. Define the input space as $\mathcal{X} = \mathcal{I} \times \mathcal{L}$, where \mathcal{I} denotes the domain of RGB images and \mathcal{L} is the linguistic (text) space. The Open-domain Visual Entity Recognition (OVEN) task seeks a function $f : \mathcal{X} \rightarrow \mathcal{E}$ which maps each image-text pair (x^p, x^t) to the unique entity $e \in \mathcal{E}$. Every entity e is associated with a Wikipedia-derived record $(t_e, I_e) \in \mathcal{K} \subseteq \mathcal{L} \times 2^{\mathcal{I}}$, where $t_e \in \mathcal{L}$ is its encyclopaedic description and $I_e \subset \mathcal{I}$ is the finite set of lead images illustrating the corresponding entity. Given a labeled training dataset $\{(x_i, e_i)\}_{i=1}^N \subset \mathcal{X} \times \mathcal{E}$, the goal is to learn a function f that minimizes the number of misclassifications.

Embeddings

Knowledge Graph Embeddings To model the knowledge existing in the knowledge graph \mathcal{G} , we adopt embedding methods to inject the knowledge into the latent space. We define knowledge graph embeddings as mappings:

$$\phi : \mathcal{E} \rightarrow \mathcal{Z}, \quad \psi : \mathcal{R} \rightarrow \mathbb{R}^{d_r},$$

where $\mathcal{Z} \subseteq \mathbb{R}^{d_e}$ is the latent space with dimension d_e . $\phi(e), \psi(r)$ are the node and relation embeddings, respectively. Common knowledge graph embedding methods define score function $f_s(e_1, r, e_2)$ to measure the plausibility of a triple $(e_1, r, e_2) \in \mathcal{T}$.

Image Embeddings Let \mathcal{I} be the space of input images. We define an image mapping function as:

$$f_\theta : \mathcal{I} \rightarrow \mathcal{Z},$$

where f_θ is represented by a deep neural network with parameters θ . Here, we leverage the pretrained frozen CLIP image encoder plus a trainable linear project layer to be f_θ .

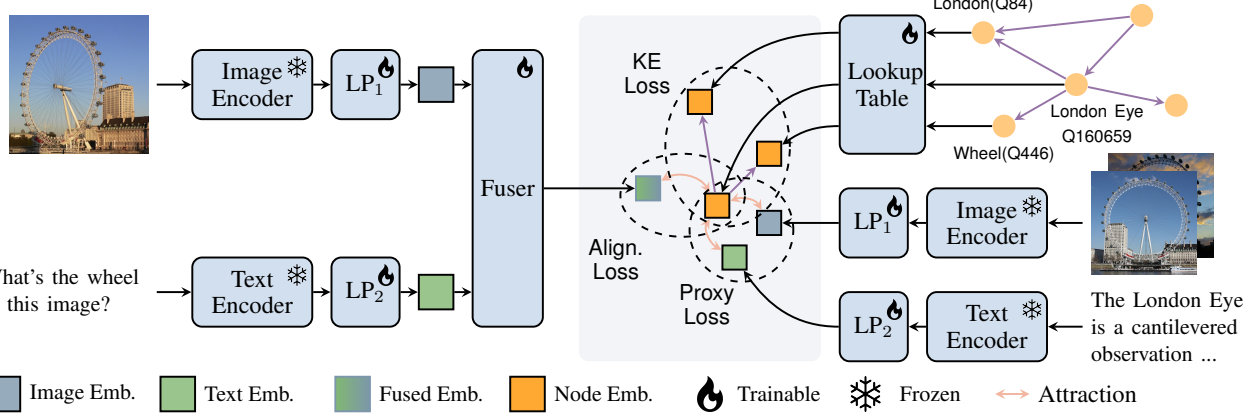


Figure 2: **Framework Overview**. Given an input image and text query (left), CLIP encoders extract image and text features. LP₁ and LP₂ present linear project layers for fine-tuning. A fuser module combines these to represent the intended entity. On the right, prior knowledge of the entity (Q160659 – London Eye)—including sample images, textual descriptions, and knowledge graph structure—is embedded using CLIP’s image and text encoders, as well as knowledge graph embedding (KGE) method. A proxy loss function is employed to align the semantic space (KGEs), visual space (image embeddings), and textual space (text embeddings). Additionally, a knowledge embedding (KE) loss is applied to learn KGEs from the structured knowledge. Finally, an alignment loss is used to align the different input representation with the corresponding entity embedding.

Text Embeddings Let \mathcal{L} be the linguistic (text) space of input text descriptions. We define a text mapping function:

$$f_\lambda : \mathcal{L} \rightarrow \mathcal{Z},$$

where f_λ is represented by a deep neural network with parameters λ . We leverage the pretrained *frozen* CLIP text encoder plus a *trainable* linear project layer to be f_λ .

We employ a dual-encoder approach to align the semantic representation of the input image and text query with that of the corresponding entity, which includes its lead image(s) and textual description. We structure our discussion into two parts: (1) encoding the input image and text query, and (2) encoding the multi-modal information of entities from the knowledge graph.

Input Image and Text Query Encoding To fuse the information of the input image x^p and the text query x^t , we employ an extra encoder

$$f_\gamma : (\mathcal{Z}, \mathcal{Z}) \rightarrow \mathcal{Z}$$

with parameters γ to fuse the image embedding $f_\theta(x^p)$ and text embedding $f_\lambda(x^t)$. The embedding, combining the information from the input image and text query, can be written as

$$\mathbf{z}^{\text{input}} = f_\gamma(f_\theta(x^p), f_\lambda(x^t)) \quad (3)$$

Entity’s Multi-modal Information Encoding For each entity e , t_e and I_e represent its text description and set of lead image(s), respectively. The entity text embedding can be written as

$$\mathbf{z}^{\text{entityText}} = f_\lambda(t_e), \quad (4)$$

and the image embedding can be written as

$$\mathbf{z}^{\text{entityImage}} = \begin{cases} \frac{1}{|I_e|} \sum_{a \in I_e} f_\theta(a) & \text{if } I_e \neq \emptyset \\ \mathbf{z}^{\text{entityText}} & \text{if } I_e = \emptyset \end{cases} \quad (5)$$

If no lead image is available for a given entity, we assign $\mathbf{z}^{\text{entityText}}$ to $\mathbf{z}^{\text{entityImage}}$. This ensures a smooth fusion of visual and textual information, as discussed in the next section.

Knowledge-guided Contrastive Learning

For given input batch $\{(x_i^p, x_i^t)\}_{i=1}^{N_b}$, where x_i^p and x_i^t are the i -th input images and its corresponding text query, N_b is the batch size, the corresponding ground truth label set is denoted as $\{e_i\}_{i=1}^{N_b}$. We define three losses, namely alignment loss, proxy loss, and knowledge graph loss, for the training process. Figure 3 shows the learning visualization.

Alignment Loss The alignment loss aims to align the joint representation of input images and text queries $\{\mathbf{z}_i^{\text{input}}\}_{i=1}^{N_b}$ with their corresponding entity representations $\{\phi(e_i)\}_{i=1}^{N_b}$. Specifically, we define the alignment loss using a contrastive objective that pulls matched embeddings closer together while pushing unmatched embeddings among the batch apart. It can be defined as

$$\mathcal{L}_a = \ell_{\text{sym}} \left(\{\mathbf{z}_i^{\text{input}}\}_{i=1}^{N_b}, \{\phi(e_i)\}_{i=1}^{N_b} \right), \quad (6)$$

where $\ell_{\text{sym}}(\cdot, \cdot)$ represents the contrastive loss function define in Equation 2.

Proxy Loss The proxy loss is defined to align the node embeddings $\{\phi(e_i)\}_{i=1}^{N_b}$ with their corresponding multi-modal representations $\{\mathbf{z}_i^{\text{entity}}\}_{i=1}^{N_b}$. This objective ensures that the node embeddings capture semantic information from both image and text modalities. It can be defined as:

$$\begin{aligned} \mathcal{L}_p = & \frac{1}{2} \ell_{\text{sym}} \left(\{\phi(e_i)\}_{i=1}^{N_b}, \{\mathbf{z}_i^{\text{entityText}}\}_{i=1}^{N_b} \right) + \\ & \frac{1}{2} \ell_{\text{sym}} \left(\{\phi(e_i)\}_{i=1}^{N_b}, \{\mathbf{z}_i^{\text{entityImage}}\}_{i=1}^{N_b} \right) \end{aligned} \quad (7)$$

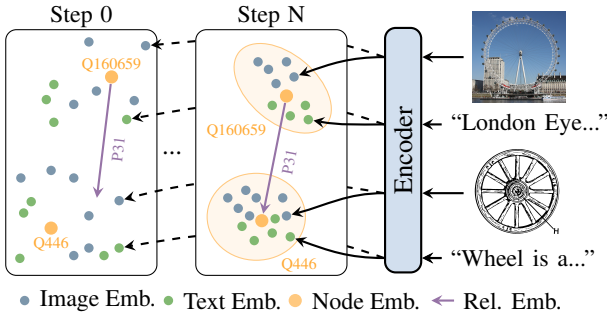


Figure 3: Node embeddings act as proxies, aligned with their corresponding image and text embeddings. Knowledge (from the KG) is captured through relational embeddings, connecting node embeddings in the latent space. Q160659, Q446, P31 represent *London Eye*, *Wheel*, and *Instance of*.

We refer to this as the proxy loss because the node embeddings serve as proxies for capturing the multi-modal semantic information of the entities. Figure 3 shows that the proxy loss gathers image and text embeddings with their corresponding node embeddings.

Knowledge Graph Embedding Loss (KE Loss) The knowledge graph loss aims to capture the structural knowledge associated with entity e_i . We first extract the triplet set associated with the entity e_i by $\mathcal{T}_{e_i} = \{(h, r, t) \in \mathcal{T} \mid h = e_i \vee t = e_i\}$. For each triplet $(h, r, t) \in \mathcal{T}_{e_i}$, we define $\mathcal{T}_{(h,r,t)}$ as the set of negative samples generated by corrupting either the head or tail entity in the positive triplet:

$$\mathcal{T}_{(h,r,t)} = \{(h', r, t) \mid h' \in \mathcal{E} \setminus \{h\}\} \cup \{(h, r, t') \mid t' \in \mathcal{E} \setminus \{t\}\}. \quad (8)$$

Based on that, the knowledge graph loss can be defined as

$$\mathcal{L}_{\text{KE}} = \sum_{i=1}^{N_b} \frac{1}{|\mathcal{T}_{e_i}|} \sum_{(h, r, t) \in \mathcal{T}_{e_i}} \frac{1}{|\mathcal{T}_{(h, r, t)}|} \left[-\log \frac{\exp(f_s(h, r, t)/\tau)}{\sum_{(h', r, t') \in \mathcal{T}_{(h, r, t)}} \exp(f_s(h', r, t')/\tau)} \right], \quad (9)$$

where τ is a temperature and $f_s(\cdot)$ is the score function defined by

$$f_s(h, r, t) = \frac{(\phi(h) + \psi(r))^\top \phi(t)}{\|\phi(h) + \psi(r)\|_2 \|\phi(t)\|_2}, \quad (10)$$

which is the cosine similarity between $\phi(h) + \psi(r)$ and $\phi(t)$. Here, we follow a translation-based KGE approach with a cosine similarity distance metric. The final loss for optimization can be defined as:

$$\mathcal{L} = \mathcal{L}_a + \beta_1 \mathcal{L}_p + \beta_2 \mathcal{L}_{\text{KE}}, \quad (11)$$

where β_1 and β_2 are two hyperparameters for balancing.

Inference

Given an input image x^p and a text query x^t , we first obtain the input embedding $\mathbf{z}^{\text{input}}$ as defined in Equation 3. The

corresponding entity answer e^* is then identified through the following inference step:

$$e^* = \arg \max_{e_j \in \mathcal{E}} \text{sim} \left(\mathbf{z}^{\text{input}}, \frac{1}{2} \left(\mathbf{z}_j^{\text{entityText}} + \mathbf{z}_j^{\text{entityImage}} \right) \right), \quad (12)$$

where $\mathbf{z}_j^{\text{entityText}}$ and $\mathbf{z}_j^{\text{entityImage}}$ denote the textual and visual embeddings of entity e_j , respectively, as defined in Equations 4 and 5.

Experiments

In our experiments, we investigate whether incorporating knowledge from large-scale KGs and Knowledge Base (KB) can enhance open-domain visual entity recognition. We analyze the impact of different types of prior knowledge, fusion methods, and KGE techniques. In addition, ablation studies on various hyperparameter values are also provided.

Experiment Settings

OVEN Dataset The OVEN dataset contains 6,063,945 training samples, which combines 14 image recognition datasets. Models are evaluated on the test splits, and performance is reported using the harmonic mean (HM) of top-1 accuracy for two types of entities: seen entities, which appear in the OVEN training set, and unseen entities, which are not present during training. Specifically, the test split includes 15,888 entities (8,355 seen and 7,533 unseen). Our evaluation is conducted solely on the OVEN benchmark, comprising 14 diverse image recognition datasets, thus indicating the generalizability of our approach. The evaluation metric is top-1 accuracy for seen and unseen entities and the HM of them.

Training details We extract a subgraph from Wikidata containing 32,122 entities and 501 relation types. For training, we use the AdamW optimizer with a learning rate of 0.001, batch size of 4096, and weight decay of 0.0001. Our approach includes three model variants based on different OpenCLIP image encoders: ViT-L/14, ViT-H/14, and ViT-bigG/14. The temperature τ for contrastive learning is fixed at 0.07 during fine-tuning. The hyperparameters β_1 and β_2 are both set to 1. We fuse information from the input image and text query (Equation (3)), using a simple *addition* operation. More details are in the Appendix.

Baselines

Dual Encoders Dual-encoder approaches consist of two encoders, each encoding a dedicated modality (e.g., images and text) into the *same* latent space. The visual recognition is conducted by searching the nearest neighbors of prototypes in the latent space for a given input image. Representative models include CLIP, CLIPfusion, and CLIP2CLIP.

Auto-regressive Captioning Another approach uses auto-regressive models to generate captions for the given images. Representative vision-language models (VLMs) such as PaLI, GIT-Large, GER-ALD, and Auto-VER follow this paradigm. These models generate a descriptive caption or name for the visual entity and then match it to the closest label in the predefined label space for final prediction.

Paradigm	Model	Venues	Parameters (B)	Pre-train Dataset	Seen	Unseen	HM
Dual-Encoder	CLIP (Radford et al. 2021)	ICML2021	0.4	OpenAI	5.6	4.9	5.2
	CLIPFusion (Hu et al. 2023)	ICCV2023	0.9	OpenAI	33.6	4.8	8.4
	CLIP2CLIP (Hu et al. 2023)	ICCV2023	0.9	OpenAI	12.6	10.5	11.4
Two-Step Generative	BLIP-v2 (Li et al. 2023a)	ICML2023	12.2	-	8.6	3.4	4.9
	PaLI-3B (Hu et al. 2023)	ICCV2023	3.0	WebLI	19.1	6.0	9.1
	PaLI-17B (Hu et al. 2023)	ICCV2023	17.0	WebLI	28.3	11.2	16.0
	GIT-Large (Caron et al. 2024)	CVPR2024	0.4	WebLI	17.6	4.3	7.0
	GER-ALD (Caron et al. 2024)	CVPR2024	0.4	LAION	29.1	16.3	20.9
	Auto-VER-7B (Xiao et al. 2024)	ECCV2024	7.0	-	62.8	16.0	25.5
Knowledge-Guided Dual-Encoder	Auto-VER-14B (Xiao et al. 2024)	ECCV2024	14.0	-	65.0	18.6	28.9
	KnowCoL-bigG(ours)	-	2.0	LAION	41.8	36.1	38.8

Table 1: Comparison with current state-of-the-art approaches on OVEN entity test split. We evaluate the harmonic mean (HM) of the seen and unseen splits (top1 accuracy) after fine tuning on OVEN training set. It serves as our main metric. The numbers of baselines are taken from papers (Caron et al. 2024; Hu et al. 2023; Xiao et al. 2024). The total parameters and pre-training datasets of the models are given for comparison.

Comparison with the state of the art We compare our proposed KnowCoL model with both dual-encoder and auto-regressive captioning baselines. As shown in Table 1, our model achieves significantly stronger performance on both seen and unseen entities. KnowCoL-bigG achieves the highest harmonic mean (HM) of 38.8%, outperforming large-scale generative models such as Auto-VER-14B and PaLI-17B despite using $7\times$ fewer parameters. We identify that the Auto-VER achieves impressive results for seen entities, but the performance significantly drops for unseen entities, indicating overfitting. Compared to theirs, KnowCoL achieves a balanced result on both seen and unseen entities, representing a strong generalization ability by including structure, textual, and visual prior knowledge.

Analysis and Ablation Studies

Here, we analyse the impact of model size, prior knowledge types, fusion strategy of the text query and input image, various KGE methods, and hyperparameters - β_1 , β_2 , latent space dimension d_e , and temperature τ . The detailed setting can be found in the Appendix section, experiment setting.

Model	Backbone	Para.(B)	Seen	Unseen	HM
CLIP	ViT-L-14	0.4	5.6	4.9	5.2
CLIPFusion	ViT-L-14	0.9	33.6	4.8	8.4
CLIP2CLIP	ViT-L-14	0.9	12.6	10.5	11.4
KnowCoL-L	ViT-L-14	0.4	34.3	29.1	31.5
KnowCoL-H	ViT-H-14	0.9	38.5	33.4	35.8
KnowCoL-bigG	ViT-bigG-14	2.0	41.8	36.1	38.8

Table 2: Comparison of model sizes. ViT-H-14 and ViT-bigG-14 are used for our KnowCoL-H and KnowCoL-bigG models. ViT-L-14 is used for CLIP, CLIPFusion, CLIP2CLIP, and KnowCoL-L. Note that CLIPFusion and CLIP2CLIP utilize two ViT-L-14 backbones.

Impact of Model Size As Table 2 demonstrates, we evaluate our model with different CLIP backbones. The backbones ViT-L-14, ViT-H-14, and ViT-bigG-14 are used for KnowCoL-L, KnowCoL-H, and KnowCoL-bigG, respectively. The performance across both seen and unseen entities consistently improves as model size increases.

We highlight that KnowCoL-L, CLIP, CLIPFusion, and CLIP2CLIP use the same backbone ViT-L-14, but KnowCoL-L significantly outperforms all. While CLIPFusion and CLIP2CLIP achieve harmonic means of 8.4% and 11.4%, respectively, KnowCoL-L reaches 31.5%, showing about 2.8 times improvement. This demonstrates that external knowledge significantly improves zero-shot generalization without increasing model size.

Model	Seen	Unseen	HM
KnowCoL-L (ViT-L-14)	34.3	29.1	31.5
w/o Lead images	32.5	27.9	30.0
w/o KG Hierarchical Knowledge	32.1	25.3	28.3

Table 3: Impact of different types of knowledge. We investigate the impact of structural knowledge, namely the Lead images in the KB and the hierarchical relations in the KG

Comparison of Knowledge Types Table 3 demonstrates the importance of different knowledge types in the KnowCoL-L model. The complete KnowCoL-L model achieves the best score of 31.5% HM. Removing lead images (w/o Lead images) reduces performance to 32.5% (seen), 27.9% (unseen), and 30.0% (HM), highlighting the role of visual context. Omitting hierarchical KG knowledge of ‘Instance of’, ‘subclass of’, and ‘parent taxon’ further lowers scores to 32.1% (seen), 25.3% (unseen), and 28.3% (HM), significantly impairing unseen entity recognition.

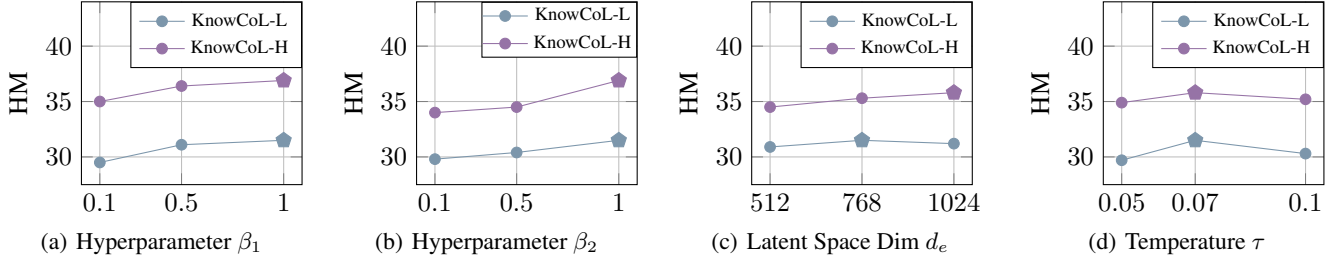


Figure 4: Ablation Studies for hyperparameter β_1 , β_2 , latent space dimension d_e , and temperature τ . HM indicates the harmonic mean of accuracies of seen and unseen entities. \blacklozenge - represents the default setting of KnowCoL approach.

Fusion Method	Layer Number	Seen	Unseen	HM
Addition	-	34.3	29.1	31.5
Concatenation + MLP	1	37.5	26.8	31.2
Concatenation + MLP	2	45.4	21.0	28.7
TE	2	54.4	16.6	25.5
TE + IP	2	56.7	17.9	27.2

Table 4: Comparison of fusion functions for combining image and text embeddings of KnowCoL-L. Our default fusion method is addition. ‘TE’ refers to the Transformer Encoder used in (Hu et al. 2023). ‘TE + IP’ is inspired by LLaVA (Liu et al. 2023). In this variant, the fusion method also incorporates local image patch tokens from the ViT encoder.

Comparison of Fusion Functions As Table 4 shows, the default Addition method provides balanced performance, achieving the best harmonic mean 31.5%. By using the multi-layer perceptron (MLP) method, the performance for seen entities improves up to 37.5%, while for unseen entities decreases to 26.8%. Using transformer encoder (TE) methods with or without local image patch embeddings significantly boost the accuracy on seen entities (54.4% and 56.7%), but degrade unseen entity recognition (16.6% and 17.9%). The trend shows that more complex fusion methods, containing more layers or a more complex structure, lead to overfitting on seen entities and sacrificing zero-shot generalization to unseen entities. Additionally, by introducing local image patch tokens (TE + IP), performance on both seen (56.7%) and unseen entities (17.9%) improves compared to the TE-only method. This improvement likely occurs because local image patch tokens provide fine-grained visual details and enhance recognition ability.

Comparison of KGE Methods Table 5 compares various knowledge graph embedding methods and distance measures. Our default choice, TransE (Bordes et al. 2013) with cosine similarity, achieves the best overall performance. This setup aligns well with CLIP, which also uses cosine similarity in its contrastive learning. When replacing the cosine similarity with Euclidean distance, the HM drops from 31.5% to 31.0%. TransH (Wang et al. 2014) introduces more representational flexibility by allowing entity embeddings to vary across different relations. This additional modeling ca-

KGE Methods	Distance Measure	Seen	Unseen	HM
TransE	Cosine Similarity	34.3	29.1	31.5
TransE	Euclidean Dis.	33.7	28.5	31.0
TransH	Cosine Similarity	34.4	28.6	31.2
DistMult	-	33.8	28.5	30.9

Table 5: Comparison of KGE methods for incorporating structural knowledge. Our default approach uses TransE combined with a cosine similarity metric. We compare this against alternative configurations, including TransE with Euclidean distance, TransH, and DistMult.

pacity slightly improved the seen performance to 34.4% but comes at the cost of lower unseen accuracy 28.6%. The DistMult method (Yang et al. 2015) shows the lowest performance, suggesting it is less effective for integrating structural knowledge from the KG into the visual-textual space.

Hyperparameters As Figure 4 shows, we conduct experiments varying the hyperparameters β_1 , β_2 , latent space dimension d_e , and contrastive learning temperature τ . Figure 4a shows that increasing the weight of the proxy loss β_1 , aligning node embeddings with multi-modal prior knowledge, enhances model performance. Figure 4b demonstrates that increasing β_2 , the weight of KE loss incorporating structured prior knowledge from Wikidata, also improves performance. Additionally, we identify that the larger model (KnowCoL-H) with more prior knowledge can benefit more from the inclusion of structured prior knowledge. Figure 4c illustrates that larger models require higher-dimensional latent spaces to represent richer features. The temperature 0.07 performs best in our task, as shown in Figure 4d.

Conclusion and Future Work

We propose KnowCoL, a novel approach to improve open-domain visual entity recognition by incorporating multi-modal prior knowledge, namely structured knowledge, textual, and visual priors. KnowCoL significantly enhances visual entity recognition performance, especially for zero-shot recognition of unseen entities. Future work includes exploring non-Euclidean spaces like hyperbolic and hyperspherical spaces to better capture the hierarchical relationships and semantic structures inherent in knowledge graphs.

Acknowledgments

The authors thank the International Max Planck Research School for Intelligent Systems (IMPRS-IS) for supporting Hongkuan Zhou, Yuqicheng Zhu, and Jingcheng Wu. This work was partially funded by the European Union’s Horizon RIA research and innovation programme under grant agreement No. 101092908 (SMARTEDGE). Jingcheng Wu has been funded by the Deutsche Forschungsgemeinschaft (DFG, German Research Foundation) - SFB 1574 - Project number 471687386. The authors also gratefully acknowledge the computing time provided on the high-performance computer HoreKa by the National High-Performance Computing Center at KIT (NHR@KIT). This center is jointly supported by the Federal Ministry of Education and Research and the Ministry of Science, Research, and the Arts of Baden-Württemberg, as part of the National High-Performance Computing (NHR) joint funding program (<https://www.nhr-verein.de/en/our-partners>). HoreKa is partly funded by the German Research Foundation (DFG).

References

Biten, A. F.; Gómez, L.; Rusiñol, M.; and Karatzas, D. 2019. Good News, Everyone! Context Driven Entity-Aware Captioning for News Images. In *CVPR*, 12466–12475. Computer Vision Foundation / IEEE.

Bordes, A.; Usunier, N.; García-Durán, A.; Weston, J.; and Yakhnenko, O. 2013. Translating Embeddings for Modeling Multi-relational Data. In *NIPS*, 2787–2795.

Bossard, L.; Guillaumin, M.; and Gool, L. V. 2014. Food-101 - Mining Discriminative Components with Random Forests. In *ECCV (6)*, volume 8694 of *Lecture Notes in Computer Science*, 446–461. Springer.

Bouarroudj, W.; Boufaïda, Z.; and Bellatreche, L. 2022. Named entity disambiguation in short texts over knowledge graphs. *Knowl. Inf. Syst.*, 64(2): 325–351.

Caron, M.; Iscen, A.; Fathi, A.; and Schmid, C. 2024. A Generative Approach for Wikipedia-Scale Visual Entity Recognition. In *CVPR*, 17313–17322. IEEE.

Chang, Y.; Cao, G.; Narang, M.; Gao, J.; Suzuki, H.; and Bisk, Y. 2022. WebQA: Multihop and Multimodal QA. In *CVPR*, 16474–16483. IEEE.

Chen, X.; Wang, X.; Changpinyo, S.; Piergiovanni, A. J.; Padlewski, P.; Salz, D.; Goodman, S.; Grycner, A.; Mustafa, B.; Beyer, L.; Kolesnikov, A.; Puigcerver, J.; Ding, N.; Rong, K.; Akbari, H.; Mishra, G.; Xue, L.; Thapliyal, A. V.; Bradbury, J.; and Kuo, W. 2023. PaLI: A Jointly-Scaled Multilingual Language-Image Model. In *ICLR*. OpenReview.net.

Chen, Z.; Chen, J.; Geng, Y.; Pan, J. Z.; Yuan, Z.; and Chen, H. 2021. Zero-Shot Visual Question Answering Using Knowledge Graph. In *ISWC*, volume 12922 of *Lecture Notes in Computer Science*, 146–162. Springer.

Farhadi, A.; Endres, I.; Hoiem, D.; and Forsyth, D. A. 2009. Describing objects by their attributes. In *CVPR*, 1778–1785. IEEE Computer Society.

Frome, A.; Corrado, G. S.; Shlens, J.; Bengio, S.; Dean, J.; Ranzato, M.; and Mikolov, T. 2013. DeViSE: A Deep Visual-Semantic Embedding Model. In *NIPS*, 2121–2129.

Goyal, Y.; Khot, T.; Agrawal, A.; Summers-Stay, D.; Batra, D.; and Parikh, D. 2019. Making the V in VQA Matter: Elevating the Role of Image Understanding in Visual Question Answering. *Int. J. Comput. Vis.*, 127(4): 398–414.

Horn, G. V.; Aodha, O. M.; Song, Y.; Cui, Y.; Sun, C.; Shepard, A.; Adam, H.; Perona, P.; and Belongie, S. J. 2018. The INaturalist Species Classification and Detection Dataset. In *CVPR*, 8769–8778. Computer Vision Foundation / IEEE Computer Society.

Hu, H.; Luan, Y.; Chen, Y.; Khandelwal, U.; Joshi, M.; Lee, K.; Toutanova, K.; and Chang, M. 2023. Open-domain Visual Entity Recognition: Towards Recognizing Millions of Wikipedia Entities. In *ICCV*, 12031–12041. IEEE.

Jeong, J.; Zou, Y.; Kim, T.; Zhang, D.; Ravichandran, A.; and Dabeer, O. 2023. Winclip: Zero-/few-shot anomaly classification and segmentation. In *Proceedings of the IEEE/CVF Conference on Computer Vision and Pattern Recognition*, 19606–19616.

Kampffmeyer, M.; Chen, Y.; Liang, X.; Wang, H.; Zhang, Y.; and Xing, E. P. 2019. Rethinking Knowledge Graph Propagation for Zero-Shot Learning. In *CVPR*, 11487–11496. Computer Vision Foundation / IEEE.

Krause, J.; Stark, M.; Deng, J.; and Fei-Fei, L. 2013. 3D Object Representations for Fine-Grained Categorization. In *ICCV Workshops*, 554–561. IEEE Computer Society.

Krishna, R.; Zhu, Y.; Groth, O.; Johnson, J.; Hata, K.; Kravitz, J.; Chen, S.; Kalantidis, Y.; Li, L.; Shamma, D. A.; Bernstein, M. S.; and Fei-Fei, L. 2017. Visual Genome: Connecting Language and Vision Using Crowd-sourced Dense Image Annotations. *Int. J. Comput. Vis.*, 123(1): 32–73.

Lampert, C. H.; Nickisch, H.; and Harmeling, S. 2009. Learning to detect unseen object classes by between-class attribute transfer. In *CVPR*, 951–958. IEEE Computer Society.

Li, J.; Li, D.; Savarese, S.; and Hoi, S. C. H. 2023a. BLIP-2: Bootstrapping Language-Image Pre-training with Frozen Image Encoders and Large Language Models. In *ICML*, volume 202 of *Proceedings of Machine Learning Research*, 19730–19742. PMLR.

Li, Z.; Tang, H.; Peng, Z.; Qi, G.-J.; and Tang, J. 2023b. Knowledge-Guided Semantic Transfer Network for Few-Shot Image Recognition. *IEEE Transactions on Neural Networks and Learning Systems*, 1–15.

Liu, H.; Li, C.; Wu, Q.; and Lee, Y. J. 2023. Visual Instruction Tuning. arXiv:2304.08485.

Maji, S.; Rahtu, E.; Kannala, J.; Blaschko, M. B.; and Vedaldi, A. 2013. Fine-Grained Visual Classification of Aircraft. *CoRR*, abs/1306.5151.

Marino, K.; Rastegari, M.; Farhadi, A.; and Mottaghi, R. 2019. OK-VQA: A Visual Question Answering Benchmark Requiring External Knowledge. In *CVPR*, 3195–3204. Computer Vision Foundation / IEEE.

Monka, S.; Halilaj, L.; and Rettinger, A. 2022. A survey on visual transfer learning using knowledge graphs. *Semantic Web*, 13(3): 477–510.

Monka, S.; Halilaj, L.; Schmid, S.; and Rettinger, A. 2021. Learning Visual Models Using a Knowledge Graph as a Trainer. In Hotho, A.; Blomqvist, E.; Dietze, S.; Fokoue, A.; Ding, Y.; Barnaghi, P. M.; Haller, A.; Dragoni, M.; and Alani, H., eds., *The Semantic Web - ISWC 2021 - 20th International Semantic Web Conference, ISWC 2021, Virtual Event, October 24-28, 2021, Proceedings*, volume 12922 of *Lecture Notes in Computer Science*, 357–373. Springer.

Nilsback, M.; and Zisserman, A. 2008. Automated Flower Classification over a Large Number of Classes. In *ICVGIP*, 722–729. IEEE Computer Society.

Norouzi, M.; Mikolov, T.; Bengio, S.; Singer, Y.; Shlens, J.; Frome, A.; Corrado, G.; and Dean, J. 2014. Zero-Shot Learning by Convex Combination of Semantic Embeddings. In *ICLR*.

Radford, A.; Kim, J. W.; Hallacy, C.; Ramesh, A.; Goh, G.; Agarwal, S.; Sastry, G.; Askell, A.; Mishkin, P.; Clark, J.; Krueger, G.; and Sutskever, I. 2021. Learning Transferable Visual Models From Natural Language Supervision. In *ICML*, volume 139 of *Proceedings of Machine Learning Research*, 8748–8763. PMLR.

Ridnik, T.; Baruch, E. B.; Noy, A.; and Zelnik, L. 2021. ImageNet-21K Pretraining for the Masses. In *NeurIPS Datasets and Benchmarks*.

Robertson, S. E.; Walker, S.; and Hancock-Beaulieu, M. 1995. Large Test Collection Experiments on an Operational, Interactive System: Okapi at TREC. *Inf. Process. Manag.*, 31(3): 345–360.

Sadikaj, Y.; Zhou, H.; Halilaj, L.; Schmid, S.; Staab, S.; and Plant, C. 2025. MultiADS: Defect-aware Supervision for Multi-type Anomaly Detection and Segmentation in Zero-Shot Learning. *CoRR*, abs/2504.06740.

Sevgili, Ö.; Shelmanov, A.; Arkhipov, M. Y.; Panchenko, A.; and Biemann, C. 2022. Neural entity linking: A survey of models based on deep learning. *Semantic Web*, 13(3): 527–570.

Singh, A.; Natarajan, V.; Shah, M.; Jiang, Y.; Chen, X.; Batra, D.; Parikh, D.; and Rohrbach, M. 2019. Towards VQA Models That Can Read. In *CVPR*, 8317–8326. Computer Vision Foundation / IEEE.

Socher, R.; Ganjoo, M.; Manning, C. D.; and Ng, A. Y. 2013. Zero-Shot Learning Through Cross-Modal Transfer. In *NIPS*, 935–943.

Wang, J.; Yang, Z.; Hu, X.; Li, L.; Lin, K.; Gan, Z.; Liu, Z.; Liu, C.; and Wang, L. 2022. GIT: A Generative Image-to-text Transformer for Vision and Language. *Trans. Mach. Learn. Res.*, 2022.

Wang, X.; Ye, Y.; and Gupta, A. 2018. Zero-Shot Recognition via Semantic Embeddings and Knowledge Graphs. In *CVPR*, 6857–6866. Computer Vision Foundation / IEEE Computer Society.

Wang, Z.; Zhang, J.; Feng, J.; and Chen, Z. 2014. Knowledge Graph Embedding by Translating on Hyperplanes. In *AAAI*, 1112–1119. AAAI Press.

Weyand, T.; Araújo, A.; Cao, B.; and Sim, J. 2020. Google Landmarks Dataset v2 - A Large-Scale Benchmark for Instance-Level Recognition and Retrieval. In *CVPR*, 2572–2581. Computer Vision Foundation / IEEE.

Xiao, J.; Hays, J.; Ehinger, K. A.; Oliva, A.; and Torralba, A. 2010. SUN database: Large-scale scene recognition from abbey to zoo. In *CVPR*, 3485–3492. IEEE Computer Society.

Xiao, Z.; Gong, M.; Cascante-Bonilla, P.; Zhang, X.; Wu, J.; and Ordonez, V. 2024. Grounding Language Models for Visual Entity Recognition. In *ECCV (11)*, volume 15069 of *Lecture Notes in Computer Science*, 393–411. Springer.

Yang, B.; Yih, W.; He, X.; Gao, J.; and Deng, L. 2015. Embedding Entities and Relations for Learning and Inference in Knowledge Bases. In *ICLR (Poster)*.

Yao, X.; Blei, T.; Meng, Y.; Zhang, Y.; Zhou, H.; Bing, Z.; Huang, K.; Sun, F.; and Knoll, A. 2025. Long-Horizon Language-Conditioned Imitation Learning for Robotic Manipulation. *IEEE/ASME Transactions on Mechatronics*, 1–12.

Zheng, L.; Chiang, W.; Sheng, Y.; Zhuang, S.; Wu, Z.; Zhuang, Y.; Lin, Z.; Li, Z.; Li, D.; Xing, E. P.; Zhang, H.; Gonzalez, J. E.; and Stoica, I. 2023. Judging LLM-as-a-Judge with MT-Bench and Chatbot Arena. In *NeurIPS*.

Zhou, H.; Bing, Z.; Yao, X.; Su, X.; Yang, C.; Huang, K.; and Knoll, A. 2024a. Language-Conditioned Imitation Learning With Base Skill Priors Under Unstructured Data. *IEEE Robotics and Automation Letters*, 9(11): 9805–9812.

Zhou, H.; Halilaj, L.; Monka, S.; Schmid, S.; Zhu, Y.; Xiong, B.; and Staab, S. 2024b. Visual Representation Learning Guided By Multi-modal Prior Knowledge. *CoRR*, abs/2410.15981.

Zhou, H.; Yao, X.; Mees, O.; Meng, Y.; Xiao, T.; Bisk, Y.; Oh, J.; Johns, E.; Shridhar, M.; Shah, D.; Thomason, J.; Huang, K.; Chai, J.; Bing, Z.; and Knoll, A. 2023. Bridging Language and Action: A Survey of Language-Conditioned Robot Manipulation. *CoRR*, abs/2312.10807.

Zhu, Y.; Groth, O.; Bernstein, M. S.; and Fei-Fei, L. 2016. Visual7W: Grounded Question Answering in Images. In *CVPR*, 4995–5004. IEEE Computer Society.

Appendix

The following sections present detailed descriptions of the datasets and training procedures for each experimental scenario. We outline the experimental settings for each variant of our approach, including different fusion strategies for image and text embeddings, the score functions employed by various knowledge graph embedding (KGE) methods, and key hyperparameters. Additionally, we introduce our approach for extracting efficient subgraphs from Wikidata. Finally, we provide representative examples of multi-modal prior knowledge utilized in our KnowCoL approach for a clearer overview. The pseudo code for KnowCoL algorithms is listed in Algorithm 2 and 3.

Experiment Setting

Dataset

OVEN dataset consists of 14 existing datasets, grounding their labels to Wikidata IDs. These 14 datasets are originally created for image recognition/retrieval and visual question answering. They are ImageNet21k-P (Ridnik et al. 2021), iNaturalist2017 (Horn et al. 2018), Cars196 (Krause et al. 2013), SUN397 (Xiao et al. 2010), Food101 (Bossard, Guillaumin, and Gool 2014), Sports100, Aircraft (Maji et al. 2013), Oxford Flower (Nilsback and Zisserman 2008), Google Landmarks v2 (Weyand et al. 2020), VQA v2 (Goyal et al. 2019), Visual7W (Zhu et al. 2016), Visual Genome (Krishna et al. 2017), OK-VQA (Marino et al. 2019), and Text-VQA (Singh et al. 2019).

Image and Text Query Fuser

In this section, we elaborate on the different fusion functions in detail, namely addition, multi-layer perception (MLP), transformer encoder (TE), and transformer encoder with image patch embeddings (TE+IP).

Addition The default fuser we used is a simple addition operation, as it shows the best generalization ability, especially for unseen entities. The fused embedding is defined as follows:

$$\mathbf{z}^{\text{input}} = f_\theta(x^p) + f_\lambda(x^t), \quad (13)$$

where $f_\theta(\cdot)$ and $f_\lambda(\cdot)$ are the image encoder and text encoder, respectively.

Multi-layer Perception (MLP) The variant Multi-Layer Perceptron (MLP) fuser first concatenates the input image embedding and the text query embedding, each of dimension d_e , into a single embedding of dimension $2 \times d_e$. An MLP encoder then reduces this embedding dimension from $2 \times d_e$ back down to d_e . When the fusion layer is set to 1, the MLP consists of a single linear layer (input dimension $2 \times d_e$, output dimension d_e) followed by a ReLU activation function. When the fusion layer is set to 2, an additional intermediate layer of dimension d_e is introduced, resulting in two linear layers, each followed by a ReLU activation. The fused embedding is represented as follows:

$$\mathbf{z}^{\text{input}} = \text{MLP}(\text{Concat}(f_\theta(x^p), f_\lambda(x^t))), \quad (14)$$

where $\text{MLP}(\cdot)$ is the function for multi-layer perception and $\text{Concat}(\cdot)$ is the function for concatenation.

Transformer Encoder (TE) The variant transformer encoder (TE) fuses the image embedding and the text embedding with a transformer encoder on top. Both embeddings are fed into the encoder, allowing them to attend to each other through self-attention. The first output embedding from the encoder is used as a global representation, capturing the fused multi-modal information.

Transformer Encoder with Image Patch Embeddings (TE + IP) Compared to the previous approach, the local image patch embeddings from the image encoder are also fed into the transformer encoder. Similarly, the first output embedding from the encoder is used as a global representation, capturing the fused information.

KGE Method Settings

Our default setting adopts the TransE method, replacing the original Euclidean distance metric with cosine similarity. The motivation for this change is that CLIP is pre-trained using cosine similarity, and adopting the same metric ensures better alignment with the embedding space learned by CLIP. Experimental results also show that using cosine similarity improves performance. Instead of using the original margin-based formulation for negative samples, we adopt a cross-entropy-based approach, which is similar to that used in CLIP, in order to ensure that the KE loss is on the same scale as the main alignment loss. The details of other settings are given as follows.

TransE + Euclidean In this setting, we adopt the original TransE method, using Euclidean distance and margin-based calculation for negative samples. The KE loss is defined as follows:

$$\mathcal{L}_{\text{KE}} = \sum_{i=1}^{N_b} \frac{1}{|\mathcal{T}_{e_i}|} \sum_{(h, r, t) \in \mathcal{T}_{e_i}} \frac{1}{|\mathcal{T}_{(h, r, t)}|} \sum_{(h', r, t') \in \mathcal{T}_{(h, r, t)}} \times \max(0, \epsilon + f_s(h, r, t) - f_s(h', r, t')), \quad (15)$$

where ϵ represents the margin and $f_s(\cdot)$ is the score function defined by

$$f_s(h, r, t) = \|\phi(h) + \psi(r) - \phi(t)\|_2. \quad (16)$$

Here, $\phi(\cdot)$ and $\psi(\cdot)$ are functions that map nodes and relation types to corresponding embeddings.

TransH + Cosine Similarity TransH is an extension for TransE, which defines relation-specific hyperplane instead of direct translation in the entity space. It can be realized by altering the score function with

$$f_s(h, r, t) = \|(\phi(h) - \mathbf{w}_r^\top \phi(h) \mathbf{w}_r + \psi(r) - \phi(t) - \mathbf{w}_r^\top \phi(t) \mathbf{w}_r)\|_2, \quad (17)$$

where \mathbf{w}_r defines the normal vector of the hyperplane. We still use the cosine similarity and cross-entropy-based approaches to conduct contrastive learning.

DistMult The score function of DistMult is defined by

$$\text{score}(h, r, t) = \phi(h)^\top \text{diag}(\psi(r)) \phi(t), \quad (18)$$

where $\text{diag}(\mathbf{r}) \in \mathbb{R}^{d \times d}$ is the diagonal matrix with $\psi(r)$ on its diagonal. Similarly, we use the cosine similarity and cross-entropy-based approaches to conduct contrastive learning.

Hyperparameters and Training Settings

The hyperparameters used for all three variants of the KnowCoL approach, namely KnowCoL-L, KnowCoL-H, and KnowCoL-bigG, are listed as follows:

KnowCoL-L We adopt the OpenCLIP ViT-L/14 image encoder as our backbone and train for 15 epochs with a batch size of 4096. Optimization is performed using AdamW (learning rate 0.0001, $\beta_1 = 1.0$, $\beta_2 = 1.0$, weight decay 1×10^{-4}) together with a cosine-annealing learning-rate schedule. We set the embedding dimension d_e to 768 and the temperature of contrastive learning τ to 0.07. In our knowledge-graph module, each entity is associated with up to 50 triplets, and we randomly sample 25 negative triplets per entity. The model was trained using 4 NVIDIA H100 GPUs, each with 80GB of memory, over a total duration of approximately 22 hours. The training was performed using mixed precision (FP16).

KnowCoL-H We adopt the OpenCLIP ViT-H/14 image encoder as our backbone. The model is trained for 20 epochs with a batch size of 4096. The AdamW optimizer is employed with a learning rate of 1×10^{-3} , cosine annealing scheduling, and weight decay of 1×10^{-4} . The hyperparameters β_1 , β_2 , latent dimension d_e , and contrastive learning temperature τ are set as 1.0, 1.0, 1024, and 0.07, respectively. For the knowledge graph, each entity is associated with at most 50 triplets, and we draw 25 negative samples per entity. The model is trained with 8 NVIDIA H100 GPUs with 80GB memory. The total training time is around 25 hours. The training was performed using mixed precision (FP16).

KnowCoL-bigG We adopt the OpenCLIP ViT-bigG/14 image encoder as our backbone. The model is trained for 25 epochs with a batch size of 4096. The AdamW optimizer is employed with a learning rate of 1×10^{-3} , cosine annealing scheduling, and weight decay of 1×10^{-4} . The hyperparameters β_1 , β_2 , latent dimension d_e , and contrastive learning temperature τ are set as 1.0, 1.0, 1024, and 0.07, respectively. For the knowledge graph, each entity is associated with at most 50 triplets, and we draw 25 negative samples per entity. The model is trained with 8 Nvidia H200 GPUs with 140GB of memory. The total training time is about 30 hours. The training was performed using mixed precision (FP16).

Structure Knowledge Extraction

Wikidata comprises billions of entities and thousands of properties, making it computationally infeasible to utilize the entire knowledge graph for model training. Moreover,

the noise within Wikidata poses an additional hurdle, potentially obstructing the learning process and affecting model performance. To mitigate this challenge, we extract a subgraph from Wikidata that encapsulates the essential information required for the OVEN benchmark. We mainly focus on the entity-to-entity relationships among all entities occurring in the OVEN benchmark, plus the hierarchical relations ‘subclass of’ (P279), ‘instance of’ (P31), and ‘parent taxon’ (P171) to preserve the structural integrity of the knowledge representation.

Algorithm 1: Subgraph Extraction from Wikidata

```

1: Given:
  • Original Wikidata KG  $\mathcal{G} = (\mathcal{E}, \mathcal{R}, \mathcal{T})$ 
  • Dataset entity set  $\mathcal{E}_{\text{data}}$ 
  • Hierarchical relations  $p_1$  (‘subclass of’),  $p_2$  (‘instance of’), and optionally  $p_3$  (‘parent taxon’).
2: Initialize  $\mathcal{E}_{\text{data}}^+ \leftarrow \mathcal{E}_{\text{data}}$ 
3: for each entity  $e \in \mathcal{E}_{\text{data}}$  do
4:   Find superclasses:  $S_e = \{e' \mid (e, p_1, e') \in \mathcal{T} \vee (e, p_2, e') \in \mathcal{T}\}$ 
5:   Update  $\mathcal{E}_{\text{data}}^+ \leftarrow \mathcal{E}_{\text{data}}^+ \cup S_e$ 
6: end for
7: Initialize  $\mathcal{T}_{\text{sub}} \leftarrow \emptyset$ ,  $\mathcal{R}_{\text{sub}} \leftarrow \emptyset$ 
8: for each triple  $(e_1, r, e_2) \in \mathcal{T}$  do
9:   if  $e_1 \in \mathcal{E}_{\text{data}}^+$  and  $e_2 \in \mathcal{E}_{\text{data}}^+$  then
10:     $\mathcal{T}_{\text{sub}} \leftarrow \mathcal{T}_{\text{sub}} \cup \{(e_1, r, e_2)\}$ 
11:     $\mathcal{R}_{\text{sub}} \leftarrow \mathcal{R}_{\text{sub}} \cup \{r\}$ 
12:   end if
13: end for
14: Define induced subgraph:  $\mathcal{G}_{\text{sub}} = (\mathcal{E}_{\text{data}}^+, \mathcal{R}_{\text{sub}}, \mathcal{T}_{\text{sub}})$ 
15: return  $\mathcal{G}_{\text{sub}}$ 

```

The Wikidata knowledge graph is denoted as $\mathcal{G} = (\mathcal{E}, \mathcal{R}, \mathcal{T})$, where \mathcal{E} , \mathcal{R} represents the entity set and predicates set, respectively. $\mathcal{T} \subseteq \mathcal{E} \times \mathcal{R} \times \mathcal{E}$ is the set of triples (e_1, r, e_2) where $e_1, e_2 \in \mathcal{E}$ and $r \in \mathcal{R}$.

The entity set of the dataset is denoted as \mathcal{E} . We first expand it by incorporating all superclasses of the entities in E , as defined by the ‘subclass of’ p_1 and the ‘instance of’ p_2 relation in Wikidata. The resulting expanded set, denoted as E^+ , is defined as:

$$\mathcal{E}_{\text{data}}^+ = \mathcal{E}_{\text{data}} \cup \{e' \mid e \in \mathcal{E}_{\text{data}}, (e, p_1, e') \in \mathcal{G} \vee (e, p_2, e') \in \mathcal{G}\}, \quad (19)$$

where e' denotes a superclass of entity e .

We define the subgraph \mathcal{G}_{sub} as the induced subgraph containing all entities in $\mathcal{E}_{\text{data}}^+$ and all relations that exist between these entities. Formally, the subgraph \mathcal{G}_{sub} is defined as:

$$\mathcal{G}_{\text{sub}} = (\mathcal{E}_{\text{data}}^+, \mathcal{R}_{\text{sub}}, \mathcal{T}_{\text{sub}}) \quad (20)$$

where

$$\begin{aligned} \mathcal{R}_{\text{sub}} &= \{r \mid \exists e_1, e_2 \in \mathcal{E}_{\text{data}}^+, (e_1, r, e_2) \in \mathcal{T}\}, \\ \mathcal{T}_{\text{sub}} &= \{(e_1, r, e_2) \in \mathcal{T} \mid e_1, e_2 \in \mathcal{E}_{\text{data}}^+ \wedge r \in \mathcal{R}\}. \end{aligned} \quad (21)$$

This subgraph \mathcal{G}_{sub} contains the relations between entities existing in the OVEN benchmark and the hierarchical relations between the entities and their super classes. The pseudo code can be seen in Algorithm 1.

Algorithm 2: Knowledge-Guided Contrastive Learning - Training

- 1: Given:
 - Dataset $D = \{(x_i^p, x_i^t, e_i)\}_{i=1}^N$
 - Knowledge Base $\mathcal{K} = \{(t_{e_i}, I_{e_i})\}_{i=1}^{|\mathcal{E}|}$, where t_{e_i} is the text description and I_{e_i} is the lead images set of entity e_i
 - Knowledge Graph $\mathcal{G} = (\mathcal{E}, \mathcal{R}, \mathcal{T})$
 - The model $\mathcal{F} = \{f_\theta, f_\lambda, f_\gamma, \phi, \psi\}$ with pre-trained image and text encoders f_θ, f_λ , fusion function f_γ , and entity and relation mapping function ϕ, ψ
- 2: Initialize projection layers of encoders f_θ, f_λ , and fusion f_γ , the other parameters of the encoders remain fixed.
- 3: Randomly initialize entity embeddings lookup table $\{\phi(e_i)\}_{i=1}^{|\mathcal{E}|}$ and relation embeddings lookup table $\{\psi(r_i)\}_{i=1}^{|\mathcal{R}|}$
- 4: **while** not converged **do**
- 5: Sample batch $\{(x_i^p, x_i^t, e_i)\}_{i=1}^{N_b}$ from D
- 6: $\mathbf{z}_i^{\text{input}} = f_\gamma(f_\theta(x_i^p), f_\lambda(x_i^t))$
- 7: $\mathbf{z}_i^{\text{entityText}} = f_\lambda(t_{e_i})$
- 8: $\mathbf{z}_i^{\text{entityImage}} = \frac{1}{|I_{e_i}|} \sum_{a \in I_{e_i}} f_\theta(a)$ if $I_{e_i} \neq \emptyset$ else $\mathbf{z}_i^{\text{entityText}}$
- 9: Compute alignment loss L_a , proxy loss L_p , and knowledge graph embedding loss L_{KE}
- 10: Compute total loss $L = L_a + \beta_1 L_p + \beta_2 L_{KE}$
- 11: Update parameters θ, λ, γ based on L
- 12: **end while**

Algorithm 3: Knowledge-Guided Contrastive Learning - Inference

- 1: Given
 - Image x^p
 - Text query x^t
- 2: Compute $\mathbf{z}^{\text{input}} = f_\gamma(f_\theta(x^p), f_\lambda(x^t))$
- 3: Return predicted entity $e^* = \arg \max_{e_j \in \mathcal{E}} \text{sim} \left(\mathbf{z}^{\text{input}}, \frac{1}{2} \left(\mathbf{z}_j^{\text{entityText}} + \mathbf{z}_j^{\text{entityImage}} \right) \right)$

Additional Experiments

The OVEN dataset consists of two splits: the entity split, derived from image recognition datasets, and the query split, originating from visual question answering datasets. In this paper, we primarily focus on the entity split. For completeness, we also show results on the query split below. We observed that the OVEN training data includes a limited amount of query split data, making this split significantly underrepresented. In the training dataset, 4,926,314 samples belong to the entity split while only 32,255 samples belong to the query split. To address this imbalance, we duplicate the query split data in each training epoch by $50\times$, which substantially improves performance on the query-based test set. We also observe that generative models such as BLIP-v2 and PaLI perform better on the query split than on the entity split, despite their inability to consistently predict the correct entity. This may be because these models are trained on visual question answering (VQA) tasks and are therefore more aligned with the query split format. Alternatively, the improved performance might be partially attributed to data leakage or overlap with the VQA-style training data.

Multi-modal Prior Knowledge of Sample Entities

Table 7 presents representative examples of prior knowledge used in the proposed model. Specifically, we provide three

Methods	Duplicate Numbers	Query Split		
		Seen	Unseen	HM
KnowCoL-L	1	8.5	6.1	7.1
KnowCoL-L	10	11.7	7.3	8.9
KnowCoL-L	50	16.2	8.0	10.7
KnowCoL-H	50	18.5	10.5	13.4
KnowCoL-bigG	50	21.7	12.1	15.6

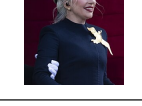
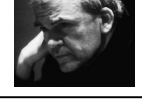
Table 6: Query Split Results

illustrative examples each for animals, cars, landmarks, and people. For each example, we include a lead image, a concise textual description, and associated structural knowledge from Wikidata. The structured relationships relevant to these entities, such as ‘instance of’ (P31), ‘subclass of’ (P279), and ‘parent taxon’ (P171), among other significant properties, are detailed in the table. This structured knowledge helps enrich entity representation, facilitating semantic disambiguation and enhancing the generalization capabilities of our KnowCoL framework.

Qualitative Analysis

To complement our quantitative evaluation, we present qualitative examples of KnowCoL’s predictions on the OVEN test set in Table 8. These cases illustrate the model’s abil-

Table 7: Prior Knowledge of Sample Entities: for each entity we show its lead image, a brief textual description, and its structural knowledge as key Wikidata triples (with that entity as **head**).

Name (QID)	Lead Image	Entity Text Description	Predicate Name (PID)	Entity Name (QID)
Mountain Hare (Q180035)		The mountain hare (Lepus timidus), also known as blue hare, tundra hare, variable hare, white hare, snow hare, alpine hare, and Irish hare, is a species of Palearctic hare that is largely adapted to polar and mountainous habitats...	Instance of (P31) Taxon Rank (P105) Parent Taxon (P171) Diel Cycle (P9566) Habitat (P2974)	Taxon (Q16521) Species (Q7432) Lepus (Q3830767) Nocturnal (Q101029366) Grassland (Q1006733)
Platypus (Q15343)		The platypus (Ornithorhynchus anatinus), sometimes referred to as the duck-billed platypus, is a semiaquatic, egg-laying mammal endemic to eastern Australia, including Tasmania. The platypus is the sole living representative of ...	Instance of (P31) Taxon Rank (P105) Parent Taxon (P171) Endemic To (P183) Characteristic (P1552)	Taxon (Q16521) Species (Q7432) Ornithorhynchus (Q3745848) Australia (Q408) Oviparity (Q212306)
Morpho Menelaus (Q545709)		The Menelaus blue morpho (Morpho menelaus) is one of thirty species of butterfly in the subfamily Morphinae. Its wingspan is approximately 12 cm (4.7"), and its dorsal forewings and hindwings are a bright, iridescent blue edged with black ...	Instance of (P31) Taxon Rank (P105) Parent Taxon (P171) Color (P462) Has Part(s) (P527)	Taxon (Q16521) Species (Q7432) Morpho (Q645804) Blue (Q1088) Insect Wing (Q276572)
BMW X5 (Q796778)		The BMW X5 is a mid-size luxury crossover SUV produced by BMW. The X5 made its debut in 1999 as the E53 model. It was BMW's first SUV. At launch, it featured all-wheel drive and was available with either a manual or ...	Instance of (P31) Manufacturer (P176) Subclass of (P279) Subclass of (P279) Subclass of (P279)	Automobile M. (Q3231690) BMW (Q26678) Executive Car (Q1357619) Car (Q1420) Road Vehicle (Q1515493)
Tesla Model S (Q1463050)		The Tesla Model S is a battery-electric, four-door full-size car produced by the American automaker Tesla since 2012. The automaker's second vehicle and longest-produced model, the Model S has both received mixed reviews from critics ...	Instance of (P31) Manufacturer (P176) Follows (P155) Followed by (P156) Subclass of (P279)	Automobile M. (Q3231690) Tesla, Inc. (Q478214) Tesla Roadster (Q210893) Model X (Q1634161) Electric Car (Q193692)
Volkswagen Beetle (Q1968742)		The Volkswagen Beetle, officially the Volkswagen Type 1, is a small family car produced by the German company Volkswagen from 1938 to 2003. One of the most iconic cars in automotive history, the Beetle is noted for its distinctive shape...	Instance of (P31) Instance of (P31) Brand (P1716) Origin Country (P495) Powered by (P516)	Automobile M. (Q3231690) Vehicle M. (Q29048322) Volkswagen (Q246) Germany (Q183) Gas. Engine (Q502048)
Taj Mahal (Q9141)		The Taj Mahal is an ivory-white marble mausoleum on the right bank of the river Yamuna in Agra, Uttar Pradesh, India. It was commissioned in 1631 by the fifth Mughal emperor, Shah Jahan to house the tomb of his beloved wife ...	Instance of (P31) Instance of (P31) Religion (P140) Country (P17) Architect (P84)	Tomb (Q381885) Tourist Attr. (Q570116) Islam (Q432) India (Q668) Ahmad Lahori (Q2551253)
Potala Palace (Q71229)		Potala Palace is the name of a museum in the Tibet Autonomous Region of China previously a palace of the Bö sovereign in Ü, the Dalai Lama, in the dzong-style, in Lhasa, capital of Bod and historically Ü. It was the winter palace of the ...	Instance of (P31) Instance of (P31) Has Use (Q71229) Different From (P1889) Country (P17)	Palace (Q16560) Tourist Attr. (Q570116) Official Resi. (Q481289) State Housing (Q7603702) China (Q148)
Faroe Islands (Q4628)		The Faroe Islands are an archipelago in the North Atlantic Ocean and an autonomous territory of the Kingdom of Denmark. Located between Iceland, Norway, and the United Kingdom, the islands have a population of 54,900 as ...	Instance of (P31) Country (P17) Part of (P361) Continent (P30) Capital (P36)	Country (Q6256) Denmark (Q35) Northern Europe (Q27479) Europe (Q46) Tórshavn (Q10704)
Stephen Curry (Q352159)		Wardell Stephen Curry II, born March 14, 1988, also known as Steph Curry, is an American professional basketball player and point guard for the Golden State Warriors of the National Basketball Association (NBA).	Instance of (P31) Sex/Gender (P21) Citizenship (P27) Occupation (P106) Father (P22)	Human (Q5) Male (Q6581097) United States (Q30) Basketball P. (Q3665646) Dell Curry (Q1184381)
Lady Gaga (Q19848)		Stefani Joanne Angelina Germanotta [a] (born March 28, 1986), known professionally as Lady Gaga, is an American singer, songwriter, and actress. She is an influential figure in popular music, known for her image reinventions and ...	Instance of (P31) Sex/Gender (P21) Citizenship (P27) Occupation (P106) Occupation (P106)	Human (Q5) Female (Q6581072) United States (Q30) Singer (Q177220) Songwriter (Q753110)
Milan Kundera (Q93166)		Milan Kundera was a Czech and French novelist. Kundera went into exile in France in 1975, acquiring citizenship in 1981. His Czechoslovak citizenship was revoked in 1979, but he was granted Czech citizenship in 2019...	Instance of (P31) Sex/Gender (P21) Citizenship (P27) Occupation (P106) Instrument (P1303)	Human (Q5) Male (Q6581097) France (Q142) Writer (Q36180) Piano (Q5994)

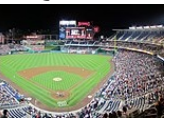
Input Image	Text Query	1	2	3	Ground Truth
	what is this building called?	Q6406516 	Q15278727 	Q7637054 	Q6406516 
	which species of insect is this?	Q5135458 	Q5379231 	Q4694221 	Q4694221 
	where is this place?	Q1014274 	Q2193788 	Q1012308 	Q2075156 
	what is the model of this aircraft?	Q6423 	Q62161 	Q852 	Q6423 
	what is the name of this park?	Q517545 	Q912770 	Q7381109 	Q517545 

Table 8: Example KnowCoL’s predictions on five test images. For each query, the model’s top-3 (according to the cosine similarity) Wikidata items predictions are shown, with green borders indicating correct matches and red borders indicating incorrect ones; the ground-truth item is in the rightmost column.

ity to recognize fine-grained entities under zero-shot settings correctly.

Overall, KnowCoL can place the correct Wikidata Q-ID at rank 1 for most cases, even though those three are drawn from a pool of more than 30000 candidates. Its main failure occurs when the top candidates are similar (e.g., different medieval ruins), causing the true entity to slip out of the top three entirely. We also observe that the top three candidates are all highly plausible alternatives to the ground truth.